Mem. S.A.It. Vol. 77, 873

Memorie della

Spectral energy distributions in presence of shells of dust around AGB stars

L. Piovan, R. Tantalo, and C. Chiosi

Department of Astronomy, University of Padova, Vicolo dell'Osservatorio 2, I-35122, Padova (Italy)
e-mail: piovan@pd.astro.it, tantalo@pd.astro.it, chiosi@pd.astro.it

Abstract. We present theoretical Spectral Energy Distributions (SEDs) of Single Stellar Populations (SSPs) of intermediate and old ages, in which the effect of the dust shells enshrouding Asymptotic Giant Branch (AGB) stars is taken into account. These dust-rich shells are produced by the stellar wind from AGB stars. They absorb the radiation coming from the star underneath and re-emit it in the mid and far infrared (MIR/FIR). To this aim, we follow in detail the evolution of the AGB stars and solve the radiative transfer equation for a realistic model of the dust shell. We show how important features of the SEDs, such as the $9.7\mu m\ Si-O$ and the $11.3\mu m\ SiC$, evolve with time. The theoretical results are compared to observational data for stars and clusters of the Magellanic Clouds.

Key words. stars: AGB – stars: mass-loss – stars: spectra – stars: dust – spectra: infrared

1. Introduction

The key tools of photometric studies are the single stellar populations (SSPs), i.e. the building blocks of star assemblies of different complexity going from star clusters to galaxies, and the fundamentals of population synthesis techniques. With a few exceptions, the light emitted by SSPs is modeled neglecting the presence of dust around their stars (Bertelli et al. 1994; Tantalo 1998, e.g.). However, there are at least two situations in which dust is present: the very initial stages when the newly born stars are still embedded in their molecular clouds, and the late stages of AGB stars when dusty envelopes are formed. The shells of dust surrounding AGB stars are the result of mass-loss by stellar winds and the complex structure and evolution of these stars during the thermally pulsing AGB phase (TP-AGB). They trap the radiation coming from the central AGB star and re-emit it in the far IR (see Habing 1996, for a classical review of this topic). The contribution to the IR radiation by the dust-enshrouded AGB stars is relevant because of the intrinsic high luminosity of these stars. Many studies have been devoted to model the circumstellar shells of AGB stars and to understand in detail the properties of the shell structure (cf. Habing 1996). However, only an handful of studies have tried to include the effect of the AGB dust shells in the SEDs of SSPs: e.g. Bressan et al. (1998), Mouhcine & Lançon (2002); Lançon & Mouhcine (2002) and Mouhcine (2002). There are several causes hampering detailed studies of the subject: (i) First of all, theoretical spectra of oxygen-rich (O-stars) and carbon-rich (C-

Send offprint requests to: L. Piovan

stars) AGB stars surrounded by shells of matter. Theoretical spectra of AGB stars of any type are particularly difficult to obtain because of the many parameters entering the problem. (ii) Second, for long time SSPs have been developed to interpret observational data in the optical range of the spectrum. Only recently the wealthy of data in the IR have spurred several groups to develop suitable SSPs extending to the MIR/FIR. The study of Bressan et al. (1998), despite some limitations such as the use of giant spectra to model the radiative transfer in O-stars and C-stars, the lack of the transition between O-stars and C-stars, and the simple treatment of the dust composition, has opened the way to a new generation of SSPs in the IR. Mouhcine & Lançon (2002) and Mouhcine (2002) have improved the situation including an empirical library of spectra of long period variables (LPV). It is important to note here that Bressan et al. (1998) made use of a fully theoretical approach, whereas Mouhcine & Lançon (2002); Mouhcine (2002) did it empirically. Our aim of is to explore further the theoretical line of work and to generate modern integrated SEDs of SSPs that (i) extend to the FIR; (ii) include state-of-the-art models of AGB stars; (iii) allow for the metallicity dependence; and finally (iv) include an accurate modelling of the dust shells.

2. Modelling the dust shells

We apply the code DUSTY by Ivezic & Elitzur (1997) to study the dust shells surrounding AGB stars. Spherical symmetry is adopted for the sake of simplicity. The key quantity we need to solve the radiative transfer problem and to calculate the emerging flux is the optical depth τ_λ of the shell. By using mass conservation law, dust-to-gas ratio and some approximations, this can be easily expressed as

$$\tau_\lambda \simeq \frac{\delta \dot{M} k_\lambda}{4\pi v} \frac{1}{r_{in}} \tag{1}$$

Subsequently, we need to link the physical quantities defining the optical depth of the dust shell (extinction coefficient k_λ, expansion velocity v, mass-loss rate $\dot{M}$, internal radius of the shell r_{in} and dust-to-gas ratio δ) to the physical quantities characterizing the AGB stars, e.g. mass M, radius R, effective temperature T_{eff}, period P of pulsation, luminosity L, and metal content Z. To this aim we have made use of (i) the Vassiliadis & Wood (1993) relationships correlating a) the expansion velocity to the pulsational period and b) period, mass and radius; (ii) the Habing et al. (1994) relation between expansion velocity, luminosity and dust-to-gas ratio; (iii) and finally, the mass loss rates of Vassiliadis & Wood (1993) and Ivezic & Elitzur (1994) for the super-wind phase (see Piovan et al. 2003, for more details). The extinction coefficients k_λ are let depend on the type of AGB star (whether O- or C-stars), and for the same type of star (either O- or C-stars) the opacities and the relative abundances of the grains are let change with the optical depth. For O-rich stars, (ratio $C/O < 1$) we adopt the grain composition of Suh (1999), using cold and warm silicates to better reproduce optically thick and thin shells. Following Suh (2002), we introduce also the optical properties of enstatite and forsterite to reproduce the crystalline silicates features. For C-rich stars (ratio $C/O > 1$) we adopt the Suh (1999, 2000) models, characterized by two components, SiC and AMC. Finally, there are a few parameters of the shell to be chosen before solving the radiative transfer equation. The distribution of the grain dimensions is expressed by the Dirac delta function $n(a) = \delta(a - a_0)$ with $a_0 = 0.1\mu m$, where a is the dimension of the grains. The dust condensation temperature T_d is assumed equal to $1000K$ for both types of grain, while we simply adopt for the density profile the power-law $\rho \propto r^{-2}$ (Suh 1999, 2000, 2002). Finally, we adopt the isochrones of Tantalo (1998) with metallicity Z=0.004, Z=0.008 and Z=0.02 and the library of stellar spectra of Lejeune et al. (1998).

3. Transition luminosities of AGB stars

As the composition of the ejecta much affect the chemistry and physics of the circumstellar shell, the transition from the O-rich (M-type with $C/O < 1$) to the C-rich objects (C-type with $C/O > 1$) deserves particular care. The

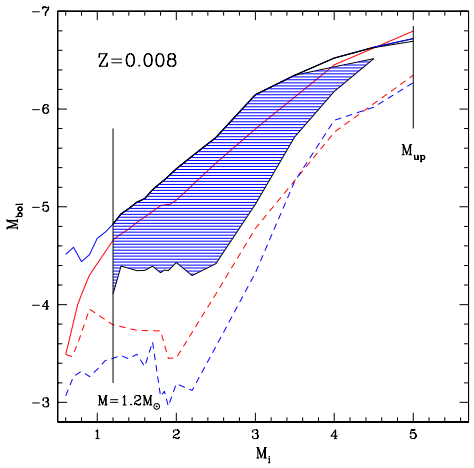

Fig. 1. The range of bolometric magnitudes spanned by AGB stars with Z=0.008 and the transition bolometric magnitudes from M- to C-star as function of the initial mass. The dashed and solid lines show the start and end of the AGB phase. The shaded area is the C-stars region. The thick lines (dashed and solid) are the models by Tantalo (1998), while the thin lines (dashed and solid) are the models by Marigo et al. (1999). The two vertical lines show the minimum mass for the formation of C-stars and the maximum mass $M_{up}$for the occurrence of the AGB phase.

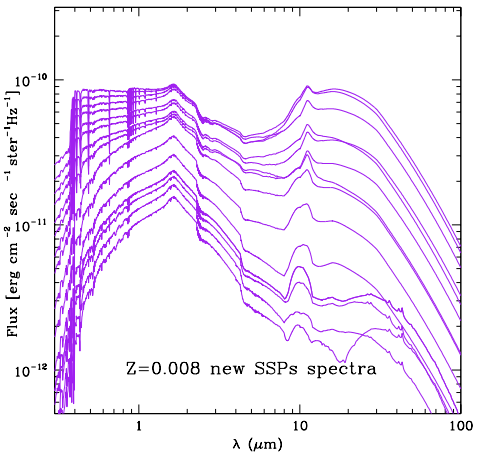

Fig. 2. SEDs F_ν vs. λ for the SSPs with Z = 0.008, ages from 0.25 to 10 Gyr and the inclusion of dusty circumstellar envelopes in AGB stars. From the bottom to the top the displayed ages are : 10, 7.5, 5, 4, 3, 2, 1.5, 1, 0.8, 0.6, 0.5, 0.4, 0.35, 0.3, and 0.25 Gyr.

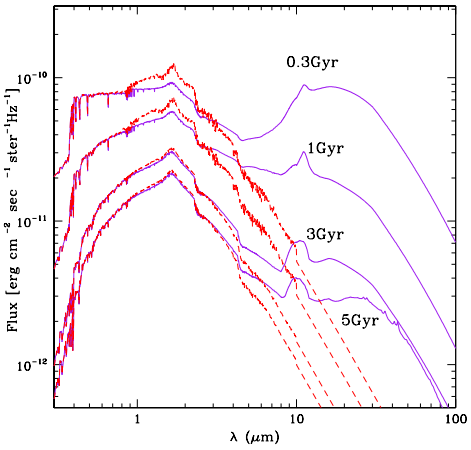

Fig. 3. Detailed comparison of SEDs F_ν vs. λ for the old (dashed lines) and new SSPs (continuous lines) with Z = 0.008. Only four ages are considered as indicated.

situation is illustrated in Fig. 1 for the Z=0.008 metallicity. It shows the bolometric magnitude of TP-AGB stars as a function of their initial mass M_i from the beginning to the end of the AGB phase when the outer envelope is completely removed by mass-loss. Over the mass interval in which the AGB phase develops, the formation of C-stars does not occur for initial masses lower than a certain limit. This is simply caused by the very early loss of the envelope before any change in the chemical composition of the outer layers may take place. Therefore, in old stars only O-rich shells of dust with $C/O < 1$ are possible. At larger initial masses, C-stars do occur over a wide range, which may extend up the maximum value for the occurrence of the AGB phase, or slightly below this. For the majority of C-stars of this metallicity the maximum luminosity coincides with the end of the AGB phase, whereas for the highest masses the maximum luminosity of C-stars can be fainter than the maximum luminosity of the AGB phase, because of envelope burning. We incorporate the results of

Marigo et al. (1999) to fix the transition luminosity along the isochrones (SSPs).

4. Infrared SEDs of SSPs

In Fig. 2 we plot the SEDs of dusty SSPs for different values of the age limited to the case with metallicity Z=0.008. A better view of the difference brought by dust is shown in Fig. 3, in which the new and old SEDs are compared for a few selected ages. The differences are remarkable.

First of all, in the old SSPs the spectra do not extend into the MIR and FIR, but sharply decline for wavelengths longer than about $3-4\,\mu m$. In contrast, the spectra of the new SSPs extend toward long wavelengths and the flux is intense also in the MIR and FIR. The differences start at about $1\mu m$ and in the IR range up to $3-4\,\mu m$ the flux of dusty SSPs is lower than the old one: this is a consequence of the fact that dust envelopes shift the emission of cold M- and C-stars toward longer wavelengths. The amount of energy shifted to longer wavelengths is larger for young ages, because more massive and luminous AGB stars are present.

It is worth noticing the different IR spectrum of the new SSPs, the evolution of the features at $11.3\,\mu m$ and $9.7\,\mu m$ in particular. For young ages the spectrum does not exhibit features due to crystalline silicates, because the C-stars dominate (the $11.3\mu m$ feature of SiC is indeed prominent); for intermediate ages, such as 3 Gyr, the O-stars of low optical depth affect the spectrum and the $9.7\,\mu m$ feature can be seen in emission. For older ages, from 5 Gyr onward, the O-stars dominate, the spectrum becomes more articulated, and the features due to crystalline silicates start to appear at long wavelengths in the IR. In Fig. 4 we plot the detailed evolution of the SiC and $Si-O$ stretching mode features at increasing age. At young ages (0.3, 0.5 Gyr) there is only the feature at $11.3\,\mu m$ of the SiC; at about at 1 Gyr, the $9.7\,\mu m$ of $Si-O$ starts to appear; in the age range 1 to 2 Gyr the two features overlap; finally, at older ages the $11.3\,\mu m$ of SiC disappears, and only the feature at $9.7\,\mu m$ of $Si-O$ occurs.

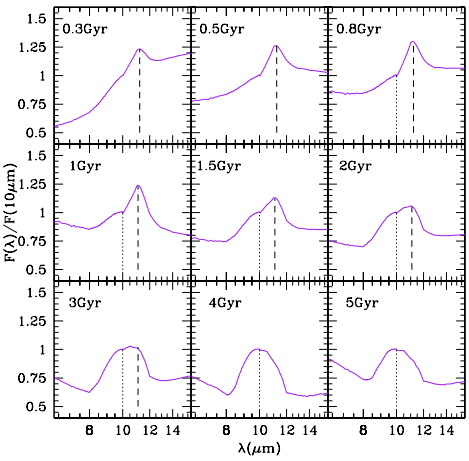

Fig. 4. Evolution of the $11.3\,\mu m$ feature (dashed vertical lines) and the $9.7\,\mu m$ feature (dotted vertical lines) in SSPs of metallicity $Z = 0.008$ and ages going from 0.3 Gyr to 5 Gyr.

5. IRAS colors of AGB stars

To test how the presence of dust shells around AGB stars would affect individual objects, we derive the IRAS colors and compare them with the observational data for a selected sample of AGB stars. Our template sample of O-rich stars (filled circles) and C-stars (open circles) is shown in the IRAS two color plane [25-60] vs [12-25] of Fig. 5. In order to show the whole range of colors spanned by these stars we make use of SSPs: the colors displayed by an SSP would correspond to AGB stars of the same age but different initial mass. In Fig.5 models of AGB stars with no dust shells around would span a small range of colors approximately centered at about around $[12-25] \simeq 0$ and $[25-60] \simeq 0$ (the encircled area displays the region covered by two SSPs with age of 0.25 and 5 Gyr). This happens because the SED of AGB stars, whose T_{eff} falls in the range 2500 to 3500 K, is much similar to the Rayleigh-Jeans black-body distribution. Therefore, it is not possible to reproduce the observational distribution of O and C-stars. Passing now to SSPs with dust enshrouded AGB stars, the situation is much improved. This is shown in Fig. 6, where now the colors of the AGB stars stretch

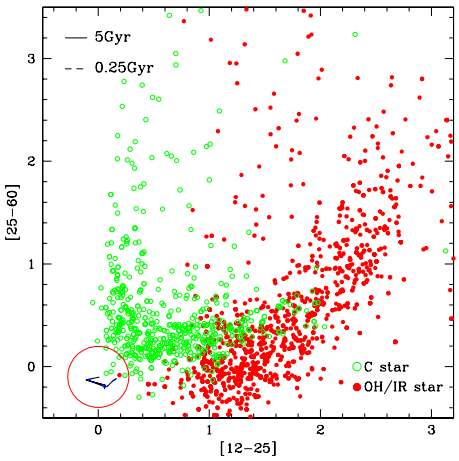

Fig. 5. The IRAS two color diagram [25 – 60] vs [15 – 25] for a sample of OH/IR-stars and C-stars. Two groups of coeval AGB stars of different mass represented by classical SSPs with age of 0.25 Gyr (dashed line) and 5 Gyr (solid line) are compared to the data. The large circle marks the color range spanned by these AGB stars.

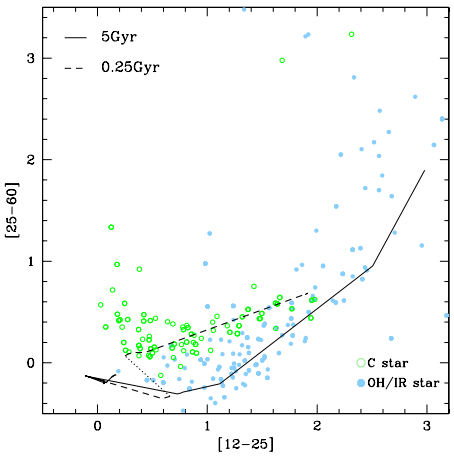

Fig. 6. The same as in Fig. 5 but using two new SSPs with age of 0.25 Gyr (dashed line) and 5 Gyr (solid line). Along the line for the young age we mark with a dotted line the rapid transition from O- to C-stars. The data have been also corrected for cirrus light contamination.

across the whole diagram. As we expect, the path in the two color plot of massive AGB stars (the young SSP of 0.25 Gyr) and low-mass AGB stars (the old SSP of 5 Gyr) is different. The low mass AGB stars overlap only the region occupied by O-stars, whereas the more massive AGB stars jump into the region crowed by C-stars when the transition from O- to C-star occurs (dotted line). The observational colours shown in Fig. 6 are also corrected for the cirrus emission C_λ known to affect the IRAS fluxes. Owing to the point-like nature of the sources, sky-subtraction may not be accurate enough and some contamination by the cirrus light can still be present. Another point to note is that our models of AGB stars of different mass do not actually cover the whole color ranges of the data, even considering the cirrus correction above. Part of the disagreement can be due to neglecting the possibility of different mixtures of silicate and carbon grains in envelopes with the same optical depth. Another possibility is that the density profile of the matter is more complicated than a continuous power-law.

6. Infrared colors of clusters

It might be worth of interest to compare the colors of SSPs with dust-enshrouded AGB stars to those of star clusters. To this aim we have looked at the young globular clusters of the Large and Small Magellanic Clouds selecting a sample in the age range in which the AGB phase can significantly contribute to the integrated light of the clusters. In Figs. 7 we show the plane $[J-H]$ vs $[H-K]$. The SSPs on display span the age range from 100-150 Myr (the first ages at which the AGB contribution is significant) to 15 Gyr and are for the metallicities $Z = 0.008$, and $Z = 0.02$. We note that both classical and new SSPs generally agree with the data, even if in the $[J-H]$ vs $[H-K]$ diagram old SSP span a narrower range in $[H-K]$ and are too red in $[J-H]$. Although the agreement is better than with the old SSPs, it is not yet satisfactory. An additional shift to bluer $[J-H]$ and $[H-K]$ is required. This would imply that the slope of

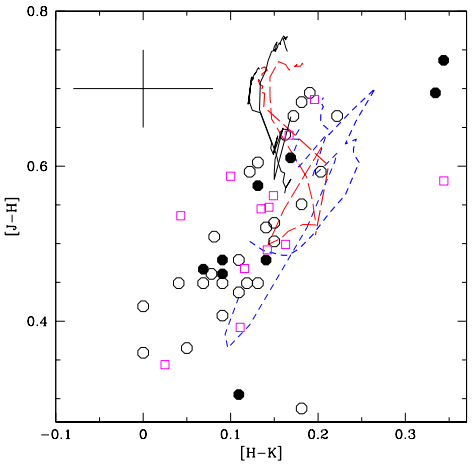

Fig. 7. The two color diagram $[J-H]$ vs $[H-K]$ for young star clusters of the Magellanic Clouds. The open circles and squares are the LMC clusters from Persson et al. (1983) and Pretto (2002), whereas the filled circles are the same but for SMC clusters. The lines show the color range spanned by SSPs of different metallicity and physical input: the thin and thick dashed lines are the SSPs of Mouhcine & Lançon (2002) for $Z = 0.02$ and $Z = 0.008$, respectively; the thin and thick long-dashed lines are our SSPs for the same metallicities; finally the thin and thick solid lines in the upper part of the diagram are the old SSPs by Tantalo (1998). The age of all SSPs is from 100-150 Myr to 15 Gyr.

the SSP SEDs ought to become steeper passing from the J to the K pass-band than allowed by the present models. Finally the SSPs by Mouhcine & Lançon (2002) extend toward bluer colors than the other SSPs. A possible explanation of this unsatisfactory fit is that the theoretical models of M giants are not yet able to reproduce the empirical spectra of O- and C-stars used by Lançon & Mouhcine (2002).

7. Conclusions

We have presented realistic SEDs of SSPs to be used in studies of the integrated colors of stellar aggregates going from star clusters to galaxies. Agreement between theory and data is good if the effect of the shells of dust around AGB stars are considered. Tabulations of SEDs are available upon request.

References

Bertelli, G., Bressan, A., Chiosi, C., Fagotto, F., & Nasi, E. 1994, A&AS, 106, 275
Bressan, A., Granato, G. L., & Silva, L. 1998, A&A, 332, 135
Habing, H. J. 1996, Astr. Astroph. Rev., 7, 97
Habing, H. J., Tignon, J., & Tielens, A. G. G. M. 1994, A&A, 286, 523
Ivezic, Z. & Elitzur, M. 1994, in ASP Conf. Ser. 64: Cool Stars, Stellar Systems, and the Sun, Vol. 8, 711
Ivezic, Z. & Elitzur, M. 1997, MNRAS, 287, 799
Lançon, A. & Mouhcine, M. 2002, A&A, 393, 167
Lejeune, T., Cuisinier, F., & Buser, R. 1998, A&AS, 130, 65
Marigo, P., Girardi, L., & Bressan, A. 1999, A&A, 344, 123
Mouhcine, M. 2002, A&A, 394, 125
Mouhcine, M. & Lançon, A. 2002, A&A, 393, 149
Persson, S. E., Aaronson, M., Cohen, J. G., Frogel, J. A., & Matthews, K. 1983, ApJ, 266, 105
Piovan, L., Tantalo, R., & Chiosi, C. 2003, A&A, 408, 559
Pretto, T. 2002, Master Thesis, University of Padova, Italy
Suh, K.-W. 1999, MNRAS, 304, 389
Suh, K.-W. 2000, MNRAS, 315, 740
Suh, K.-W. 2002, MNRAS, 332, 513
Tantalo, R. 1998, PhD thesis, Univ. of Padova
Vassiliadis, D. A. & Wood, P. R. 1993, ApJ, 413, 641